Rapid Finite-Fault Earthquake Information from Seismic and Geodetic Observations
Final Project Report

U.S.G.S Award Number 05HQGR0052; 04 HQ GR 0043; 04 HQGR0044

Mark H. Murray and Douglas S. Dreger
University of California, Berkeley, California, 94720
Ph. (510)643-1719; Fax (510)643-5811; dreger@seismo.berkeley.edu

Introduction

This project investigated the implementation of realtime processing of GPS data to be used in the automated finite-source inversion method in operation at the Berkeley Seismological Laboratory (BSL). Finite-source parameters obtained from seismic waveform or GPS data, or jointly, may be used to improve ShakeMap reporting in areas that might not have suitable near-fault strong motion instrumentation, or in cases where strong motion data might not be available due to interrupted telemetry or other issues related to the earthquake emergency. Thus the objective was to develop a series of analysis techniques and methods that operate together and independently in order to improve the redundancy and the robustness of the system.

Approach

GPS Processing

We investigated methods for processing realtime GPS observations using the GAMIT/GLOBK analysis software, which is primarily designed for static observations. We developed and implemented at the BSL a rapid processing system that determined independent hourly position estimates for realtime GPS at 20 stations in northern California. We began integrating results from this system with the realtime earthquake notification system jointly operated by the BSL and USGS using earthquake information to trigger the estimation of GPS-derived coseismic static offsets. We also investigated higher sampling rate (1 Hz) GPS processing, particularly with the recently developed Track module of GAMIT/GLOBK that uses Kalman filtering techniques to perform kinematic solutions. We found that this module offers improved ambiguity resolution using short data intervals, and works well for networks with small interstation distances, such as for stations near the M7.1 1999 Hector Mine and M6 2004 Parkfield earthquakes, but has less success on more widely spaced networks, such as the continuous GPS stations in the vicinity of the M7.9 2002 Denali earthquake.

Joint Finite-Source Inversion

We developed an automated finite-source inversion procedure, which is used to determine the slip distribution of large earthquakes rapidly after their occurrence (Dreger and Kaverina, 2000; Dreger et al., 2005). This method is based on the approach developed by Hartzell and Heaton (1983) and is capable of inverting both seismic waveform and geodetic data either independently or jointly. We have applied rapidly determined GPS data in studies of recent

earthquakes such as the 2003 San Simeon and 2004 Parkfield events as described in the results section. This same code can be used to simulate strong ground motions from a slip model. We developed a method in which slip models obtained geodetically may be used to simulate strong ground motions. We tested the approach using the strong motion data set from the 1994 Northridge, California, Mw6.7 earthquake.

Results

GPS Processing

We used both the rapid one-hour and 1-Hz kinematic techniques to estimate sub-daily coseismic and post-seismic displacements of the 2004 Parkfield earthquake (Langbein et al., 2005; Dreger et al., 2005). Our attempts to develop more realtime systems were hampered by the limitations of the GAMIT/GLOBK software and investigations by Ken Hudnut, our USGS collaborator, of more commercially available processing options were not fruitful.

Layered Elastic Inversion Code

As part of this project we updated the finite-source inverse code to incorporate layered elastic structure for the modeling of the geodetic data. The previous version of the code (Dreger and Kaverina, 2000; Kaverina et al., 2002; Dreger et al., 2005) utilized the half-space method of Okada (1985). The new code is now able to invert geodetic data using the same layered elastic structure used for the seismic waveform data using the code of Wang et al. (2006).

Inversion of 2003 San Simeon Mw6.5 Earthquake

Rolandone et al. (2006) present results of geodetic only, and joint inversions using the new layered elastic code. A copy of this paper is in the appendix.

Inversion of the 2004 Parkfield Mw6.0 Earthquake

Rapidly determined GPS data was used to characterize the rupture process of the 2004 Parkfield earthquake. We reported the preliminary results in two papers (Langbein et al., 2005; and Dreger et al., 2005). A reprint of Dreger et al. (2005) is included in the appendix. Kim and Dreger (2007) builds on the preliminary investigations of the Parkfield earthquake and includes a thorough analysis of model resolution and uncertainty.

Simulation of Strong Ground Motion from Geodetic Slip Models

GPS data can be used to independently determine the faulting orientation and slip distribution. We developed a rapid-processing system for realtime GPS data that could detect several cm-level coseismic surface displacements (typically caused by M>6 earthquakes) within ~20 minutes of the event. Our simulations suggest that simple rectangular dislocation models of fault geometry and uniform slip could be estimated using Monte Carlo non-linear inversion techniques several minutes after estimating the coseismic displacements. Such GPS slip models give no information on the timing of the slip, which is required in order to simulate

near-fault strong ground motions. The GPS slip models can be used directly by providing information on the finite extent of the fault rupture, or by interpreting the relative position of the seismically determined hypocenter with respect to the slip distribution an idea of the degree of directivity. GPS slip models cannot be used to directly simulate near-fault strong ground motions, and in order to do so a method for describing the rupture kinematics is needed. In the following we present a method of generating a kinematic model of the fault process based on the slip distribution from the inversion of GPS static displacements.

Our method for deriving a spatio-temporal slip model from static dislocations is based on the intuitive assumption that larger slip takes longer time to accumulate. This assumption follows from a self-similar scaling relation between rise time and slip in which there is constant stress drop or slip velocity. Somerville et al. (1999) provided empirical scaling relations between dislocation rise time, average slip and moment for crustal earthquakes. We obtain a constant slip velocity of 76.8 (cm/s) from their self-similar relations. This value is consistent with average values obtained assuming a constant stress drop of 30 to 100 bars.

We use the multiple time windows method of *Hartzell and Heaton* (1983) to simulate the strong ground motion time histories. Here we assume a slip distribution obtained geodetically, and then parameterize the rupture velocity and the spatially variable rise time. A minimum rise time is defined as half the rise time from the empirical relationship of Somerville et al. (1999), $T_r = 4.37\times10^{-7} M_o^{1/3}$ (here the unit of seismic moment is N·m). M_o is obtained from the geodetic slip inversion. Variable rise time over the fault surface is then defined by dividing the slip at each location by assumed constant slip velocity and then distributing uniformly over multiple staggered time windows each with a duration of $T_r/2$. The regions with smallest slip take the minimum rise time to finish slipping, while the regions with larger slip require multiple time windows (Figure 1).

In the model a circular rupture front initiates at the hypocenter and propagates with constant assumed rupture velocity. Slip is triggered when the rupture front reaches each point source and has a duration determined by the number of time windows appropriate for the level of slip at that point. We assume the hypocenter is known a priori from seismic estimates. For events in California, the hypocenter is typically determined within 30–120 seconds after the occurrence of the earthquake (*Gee et al.*, 2003). Substantially before near-realtime GPS data would be available for processing. Although it is impossible to know a priori how the rupture velocity will vary or what it will be on average, a commonly reported value is approximately 80–90% of the shear wave velocity.

We demonstrate the method by simulating PGV ShakeMaps from three slip models for the 17 January 1994 M_w 6.7 Northridge earthquake. Model REF (reference), determined by inverting near-source strong ground motions, P and SH teleseismic body waves, and GPS and spirit leveling geodetic data (*Wald et al.*, 1996), provides reference PGV for comparison with PGV obtained from the source models inferred from geodetic data only. Model UNI was obtained by a non-linear inversion method for fault orientation, dimension and uniform slip using 10 GPS displacement vectors measured in the first week after the mainshock (*Hudnut and Murray*, pers. comm., 1994). Model VAR was obtained from a non-linear inversion for fault plane geometry

followed by a linear inversion for variable slip on the estimated fault plane (Figure 1, *Hudnut et. al.*, 1996).

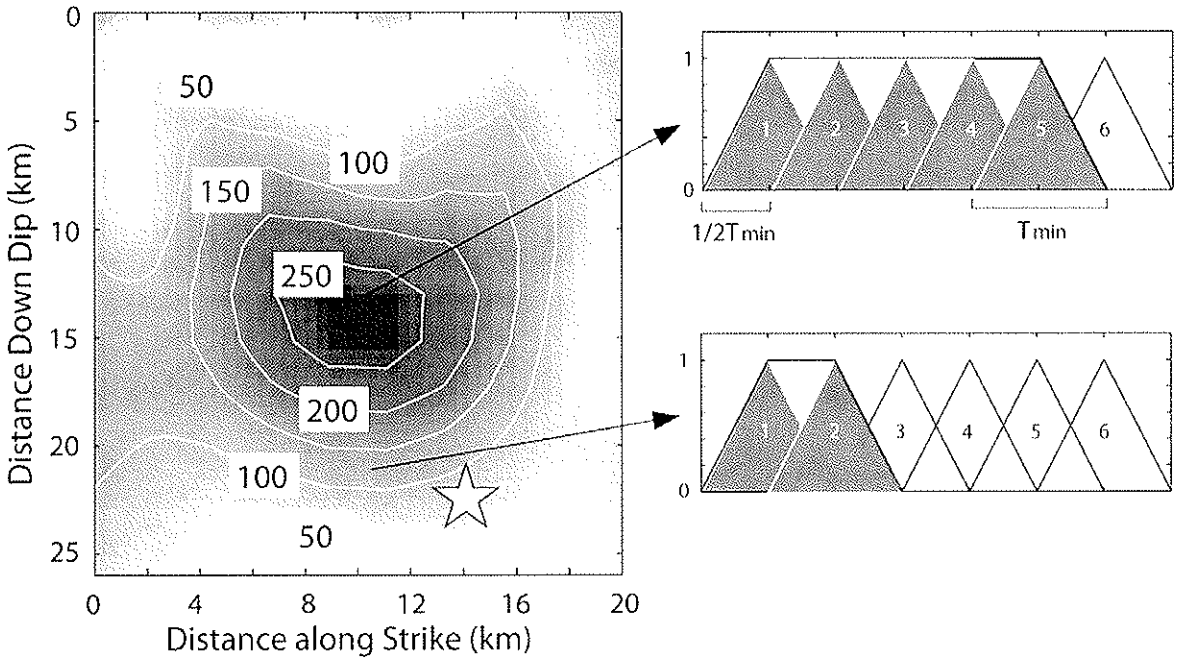

Figure 1. A schematic diagram showing how to determine the number of time windows for a variable-slip model. Left column shows the variable slip model on its rupture plane (*Hudnut et al.*, 1996). White star indicates hypocenter of Northridge event. Two small panels on the right indicate necessary time windows (solid gray triangles) and final rise time curve (thick black) associated with slip patches indicated on slip distribution model.

We assume that rupture initiated near the hypocenter (34.206°N, 118.550°W, 17.5 km depth) obtained independently from the short-period seismic network (*Hauksson et al.*, 1995). Because the fault planes used in the two geodetic slip models do not include the hypocenter, we initiated rupture at the point of intersection of a vertical line from the seismic hypocenter on the geodetic-derived fault planes. If the fault plane is too small to include the point of intersection, we extended the fault plane to include the point but no slip is assumed on the extended part of the fault. Future applications can solve for finite-source parameters with the constraint that the fault plane must include the hypocenter. We assume that the constant slip velocity is 76.8 cm/s. The two geodetic models UNI and VAR have seismic moments of 1.3715×10^{19} and 1.8985×10^{19} N·m corresponding to minimum rise time functions of 0.523 and 0.583 seconds, respectively. Given the maximum slip in each of these models (452.13 and 281.01 cm), 22 and 12 time windows are used in each model to distribute the slip in time. The final rise time as parameterized can differ from the estimated rupture time (dividing slip by slip velocity) because of the fixed duration of the unit time window. However this difference has no significant impact on the simulated ground motions. For model REF, we used the parameters for rise time and the slip-time-window distribution reported by *Wald et al.* (1996). To reduce artifacts from coarse discretization, the slip models were interpolated so that the rupture time across a subfault is much less than the minimum rise time. The final spatio-

temporal slip models have the same scalar seismic moments and slip distribution derived from the geodetic inversions, but have that slip distributed in time.

To assess the methodology, we compare predicted PGV for model REF and other two GPS-only models (VAR and UNI) at an artificial grid in the region (34-35N and 118-119E) with the interspacing of 0.1 deg in both longitude and latitude. The waveforms for each source model were simulated using Green's function for *Wald et al.*'s (1996) rock model that has a minimum shear wave velocity of 1 km/s. A predicted waveform is low-pass filtered with the corner frequency of 1 Hz. PGV is computed by taking geometric mean of two horizontal peak ground velocities at grid points. We chose to use the geometric mean of the horizontal components, because attenuation models of ground motions commonly give results in terms of the geometric mean. Predictive maps of the maximum ground motion from an individual component in the manner used in ShakeMap (Wald et al., 1999) produces similar results. To quantify our assessment, we calculated the best fitting lines of simulated PGV for model VAR and UNI as a function of predicted PGV for model REF. The slopes of the best fitting lines are 0.30 and 1.16 for models UNI and VAR. The PGV values derived from model UNI are significantly less than the predicted PGV from model REF, which is inverted from seismic waveforms, possibly because the model is too smooth and spread in time. The simulated PGV for model VAR tends to be slightly larger than model REF, but the difference is not significant (Figures 2a and 2b). This assessment indicates that even though the real slip velocity is not constant over the fault plane, the level of shaking around the fault plane can be, to a large extent, estimated by only assuming constant slip velocity derived from empirical relations.

We tested the sensitivity of the simulated PGV for model VAR to slip velocity by assuming 30, 50, 76.8, and 100 cm/s, and a constant rupture velocity of 3.0 km/s (86 % of assumed 3.5 km/s shear wave velocity) (Figure 2c). For a given rupture velocity, the level of PGV increases with slip velocity and slip velocity between 50 and 76.8 cm/s agree well with the predicted level of PGV for model REF. We also tested the sensitivity of PGV to the assumed rupture velocity for a constant slip velocity of 76.8 cm/s using 1.80, 2.45, and 3.15 km/s, which are 50, 70 and 90% of the shear wave velocity (Figure 3d). The level of PGV increases with rupture velocity and rupture velocity between 70 and 90% of shear wave velocity are appropriate to predict the level of PGV for model REF.

We estimated the time varying slip model and the predicted PGV for a given model is comparable to PGV for the model directly derived from seismic data. We compared predicted PGV for our estimated slip model to real observed PGV. As we mentioned before, it is important to have good Green's functions to predict waveforms. However, we are just interested in the level of PGV rather than waveform itself. Therefore we just use 1-D Green's functions for a rock model (*Wald et al.*, 1996) and then correct PGV for site effects.

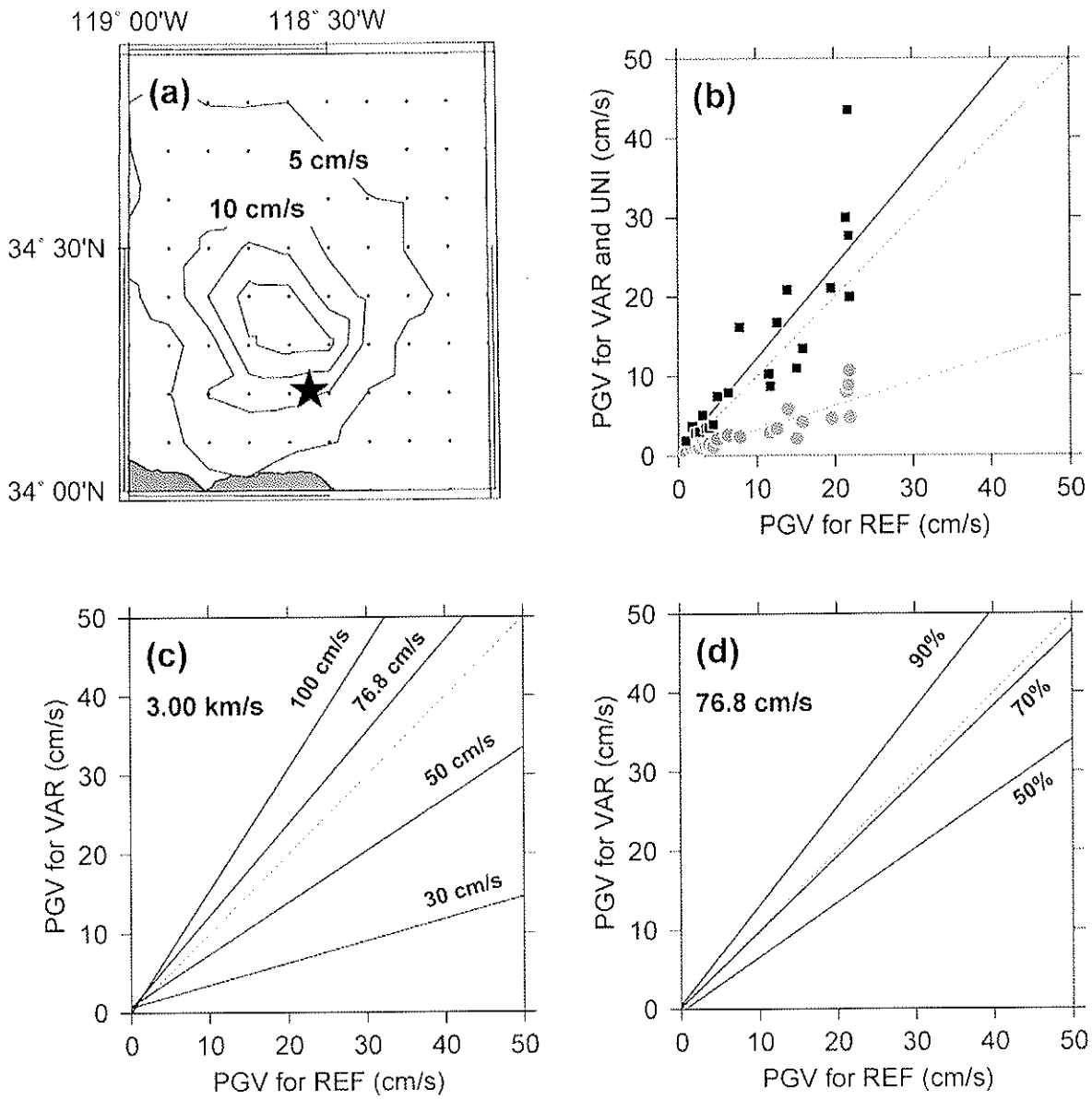

Figure 2. (a) A predicted PGV ShakeMap for model REF. The black dots are the grid locations where strong motions are derived for ShakeMap. The black star indicates mainshock epicenter. (b) A comparison of PGV for two geodetic models (VAR and UNI) and model REF. For the reference, the perfect agreement line is indicated with the dotted gray line. (c) The best fitting lines assuming different slip velocities for constant rupture velocity of 3.0 km/s. (d) The best fitting lines assuming different rupture velocities for constant slip velocity of 76.8 cm/s.

To account for site effects, we applied site amplification factors to the waveforms based on the upper 30 m shear wave velocity (*Wills et al.*, 1999) as is done in the NEHRP site classification system. Amplification factors are calculated by considering differences in impedances at surface for the rock model and given site for a normal incidence seismic wave.

$$A = \frac{2\rho_r\beta_r}{\rho_s\beta_s + \rho_r\beta_r},$$

where A is amplification factor. ρ_r and ρ_s are density at the surface and β_r and β_s are shear wave velocity at the surface for Wald's rock model (1.8 g/cm^3 and 1.00 km/s) and given site, respectively. Here density at given site is determined following empirical relations (*Brocher*, 2005; see his equations (1) and (9)). Simulated PGV ShakeMaps for model VAR within a constant slip velocity of 76.8 cm/s and rupture velocity of 3.00 km/s assumptions, derived from the geometric mean of the two horizontal-component synthetic velocities and corrected for amplification factors, were compared to observed PGV at 12 stations around the epicenter (Figure 3). The comparison shows that predicted PGV agree well with observed PGV except a couple of southern stations to the epicenter, where observed PGV is larger than predicted PGV by a factor of at least 3 (Figure 3d). This discrepancy is likely due to very complex 3-D wave propagation related with Los Angeles basin, which is not taken into account in this study.

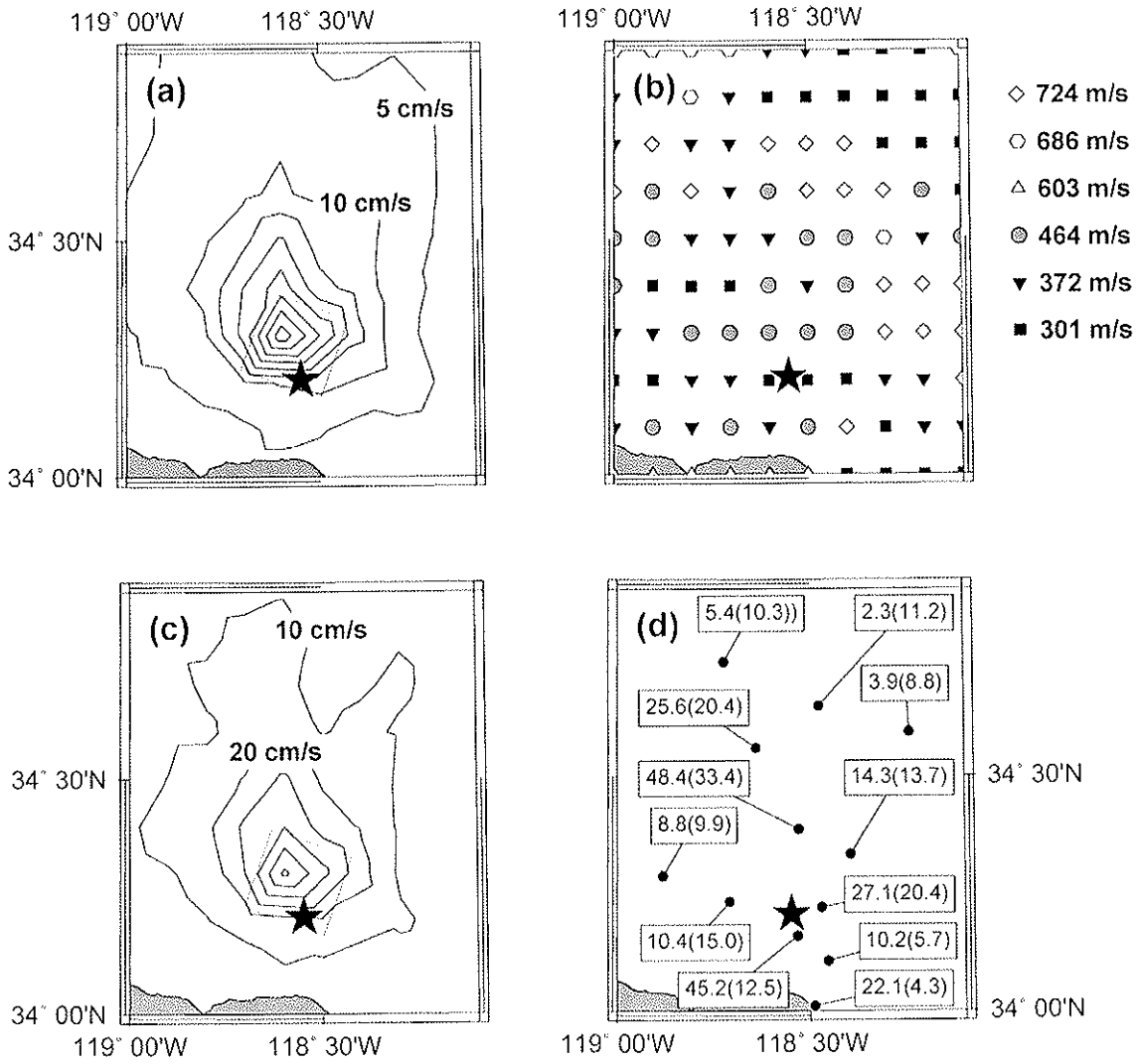

Figure 3. (a) A predicted PGV ShakeMap for model VAR within a slip velocity of 76.8 cm/s and rupture velocity of 3.00 km/s assumptions. The black star indicates mainshock epicenter. Rectangles are surface projection of model VAR. (b) An average upper 30 meter shear wave velocities at grid points within given region. (c) Same as (a) for after correcting site effects. (d) A comparison of predicted PGV and observed PGV at 12 stations. Figures in box and parenthesis refer to observed and predicted PGV in cm/s.

To summarize, we have developed a methodology to derive PGV ShakeMaps from geodetic finite-source models. Since our objective was to develop a method that is practical in a rapid (on the order of 30 minutes) post-earthquake time frame, we made several simplifying assumptions such as constant slip and rupture velocity. As more information becomes available following an earthquake it may be possible to invert for models to resolve these parameters, but such analysis is not applicable in an automated fashion. Nevertheless, to first order, assuming rupture and slip velocities are constant performs well in describing the overall

directivity effect and in simulating peak ground velocity for ShakeMap purposes (e.g., *Dreger and Kaverina*, 2000; *Dreger et al.*, 2005).

PGV for model UNI, which concentrates slip into a smaller source, tends to underpredict PGV due to both the smooth rupture and long rise time, however such a model is still useful to define source finiteness and directivity, which can be used to update ShakeMaps by correcting distance measures for finiteness or attenuation relations for directivity (e.g., *Somerville et al.*, 1997). Simulated PGV ShakeMaps for model VAR are in good agreement with the general distribution of observed PGV.

Future work will test this methodology for other large, well-studied events, such as 2003 San Simeon, 1992 Landers, and 2004 Parkfield, to optimize the rules for time variation of slip. Combining the optimized rules and near real-time measurement and inversion of GPS displacement vectors can reduce the estimation time of the extent of near-fault strong ground shaking, and thus could facilitate better emergency response activities.

References

Dreger, D., and A. Kaverina (2000) Seismic remote sensing for the earthquake source process and near-source strong shaking: A case study of the October 16, 1999 hector mine earthquake, Geophys. Res. Lett., 27, 1941-1944.

Dreger, D. S., L. Gee, P. Lombard, M. H. Murray, and B. Romanowicz (2005), Rapid Finite-Source Analysis and Near-Fault Strong Ground Motions – Application to the 2003 Mw6.5 San Simeon and 2004 Mw6.0 Parkfield Earthquakes, Seismo. Res. Lett. 76, 40-48.

Gee, L., D. Neuhauser, D. Dreger, R. Uhrhammer, M. Pasyanos, and B. Romanowicz, (2003), The rapid earthquake data integration project, International Handbook of Earthquake and Engineering Seismology, Volume 81B, p 1261-1273.

Hartzell, S. H., and T. H. Heaton (1983) Inversion of strong ground motion and teleseismic waveform data for the fault rupture history of the 1979 Imperial Valley, California, earthquake, *Bull. Seism. Soc. Am.*, 73, 1553-1583.

Hauksson, E., L. M. Jones, K. Hutton (1995), The 1994 Northridge earthquake sequence in California: Seismological and tectonic aspects, *J. Geophys. Res.*, *100*(B7), 12,335-12,355.

Hudnut, K. W., Z. Shen, M. Murray, S. McClusky, R. King, T. Herring, B. Hager, Y. Feng, A. Donnellan, and Y. Bock (1996), Co-seismic displacements of the 1994 Northridge, California, earthquake, *Bull. Seismol. Soc. Am., 86,* S19-S36.

Kaverina, A., D. Dreger, and E. Price (2002) The combined inversion of seismic and geodetic data for the source process of the 16 October 1999 M_W 7.1 Hector Mine, California, Earthquake, Bull. Seism. Soc. Am., vol.92, no.4, pp.1266-1280.

Kim, A., and D. Dreger (2007). Rupture process of the 2004 Parkfield earthquake from near-fault seismic waveform and geodetic observations, *submitted J. Geophys. Res.*

Langbein, J., D. Dreger, J. Fletcher, J. L. Hardebeck, M. Hellweg, C. Ji, M. Johnston, J. R. Murray, R. Nadeau, M. J. Rymer, and J. A. Treiman, Preliminary report on the 28 September 2004, M 6.0 Parkfield, California earthquake, Seismol. Res. Lett., 76(1), 10–26, 2005.

Okada, Y., Surface deformation due to shear and tensile faults in a half-space, *Bull. Seism. Soc. Am., 75*, 1135-1154, 1985.

Rolandone, F., D. Dreger, M. Murray, and R. Bürgmann (2006), Coseismic slip distribution of the 2003 M 6.6 San Simeon earthquake, California, determined from GPS measurements and seismic waveform data, *Geophys. Res. Lett.*, 33, L16315.

Somerville, P. G., N. F. Smith, R. W. Graves, and N. A. Abrahamson (1997), Modification of empirical strong ground motion attenuation relations to include the amplitude and duration effects of rupture directivity, *Seism. Res. Lett.*, *68*, 199-222.

Somerville, P., K. Irikura, R. Graves, S. Sawada, D. Wald, N. Abrahamson, Y. Iwasaki, T. Kagawa, N. Smith, and A. Kowada (1999), Characterizing crustal earthquake slip models for the prediction of strong ground motion, *Seism. Res. Lett., 70,* 59-80.

Wald, D., and T. Heaton (1994), Spatial and temporal distribution of slip for the 1992 Landers, California, earthquake, *Bull. Seism. Soc. Am.*, *84*, 668-691.

Wald, D. J., T. H. Heaton, and K. W. Hudnut (1996), The slip history of the 1994 Northridge, California, earthquake determined from strong-motion, teleseismic, GPS, and leveling data, *Bull. Seism. Soc. Am., 86,* S49-S70.

Wang, R., F.L. Lorenzo Martin, and F. Roth (2006), PSGRN/PSCMT – a new code for calculating co- and post-seismic deformation, geoid and gravity changes based on the viscoelastic-gravitational dislocation theory, *Comp. Geosci.*, **32**, 527-541.

Wills, C. J., M. Petersen, W. A. Bryant, M. Reiche, G. J. Saucedo, S. Tan, G. Taylor, and J. Treiman (2000), A Site-Condistions Map for California Based on Geology and Shear-Wave Velocity, *Bull. Seism. Soc. Am., 90*, S187-S208.